

Complexity Reduced QRM-ML Block Signal Detections for Single-carrier Transmission

Tetsuya YAMAMOTO[†] Kazuki TAKEDA[†] and Fumiyuki ADACHI[‡]

Dept. of Electrical and Communication Engineering, Graduate School of Engineering, Tohoku University
6-6-05 Aza-Aoba, Aramaki, Aoba-ku, Sendai, 980-8579 Japan

[†]{yamamoto, kazuki}@mobile.ecei.tohoku.ac.jp, [‡]adachi@ecei.tohoku.ac.jp

Abstract - Maximum likelihood block signal detection with QR decomposition and M-algorithm (QRM-MLBD) can significantly improve the bit error rate (BER) performance of cyclic prefix-added single-carrier (CP-SC) block transmission when compared to the frequency-domain equalization (FDE) based on the minimum mean square error (MMSE) criterion. However, in order to achieve the sufficiently improved performance, a fairly large number M of surviving paths in the M-algorithm is required. Recently, to solve this problem, we proposed two types of complexity reduced QRM-MLBD schemes. The first one is MMSE QRM-MLBD. The second one is training sequence-aided QRM-MLBD. In this paper we compare above two complexity reduced QRM-MLBDs in terms of BER performance and computational complexity.

I. INTRODUCTION

When the single-carrier (SC) transmission without any equalization technique is used, the bit error rate (BER) performance significantly degrades due to strong inter-symbol interference (ISI) in a severely frequency-selective channel [1].

Recently, a near maximum likelihood (ML)-based reduced complexity frequency-domain equalization scheme, which is called QR decomposition with M-algorithm ML block signal detection (QRM-MLBD), was proposed for the reception of cyclic prefix-added single-carrier (CP-SC) signals [2, 3]. In QRM-MLBD, QR decomposition is applied to a concatenation of the propagation channel and discrete Fourier transform (DFT). We showed [3] that QRM-MLBD can significantly improve the BER performance when compared to the frequency-domain equalization (FDE) based on the minimum mean square error (MMSE) criterion [4] and achieve the BER performance close to the matched filter (MF) bound even if high level data modulation is used. However, a fairly large number M of surviving paths in the M-algorithm is required, leading to high computational complexity.

Recently, to solve this problem, we proposed two types of complexity reduced QRM-MLBD schemes. The first one is the application of MMSE QRM-MLBD, which was originally proposed for multi-input multi-output (MIMO) spatial multiplexing [5], to the SC block signal detection [6]. The second one is training sequence (TS)-aided QRM-MLBD [7]. In TS-aided QRM-MLBD, the TS-added SC (TS-SC) block transmission [8] is used instead of CP-SC block transmission. In TS-SC block transmission, CP is replaced by a known TS,

which is a part of DFT block at the receiver, and TS in the previous block acts as CP in the present block.

In this paper, we compare our previously proposed complexity reduced QRM-MLBDs in terms of BER performance and computational complexity. The remainder of this paper is organized as follows. Sect. II presents CP-SC and TS-SC transmission system model. In Sect. III, QRM-MLBD for CP-SC and MMSE QRM-MLBD are presented. In Sect. IV, TS-aided QRM-MLBD is presented. In Sect. V, we will discuss the BER performance and computational complexity comparison of above two complexity reduced QRM-MLBD. Sect. VI offers some concluding remarks.

II. CP- AND TS-SC TRANSMISSION SYSTEMS

A. CP-SC

The CP-SC block transmission system model and the CP-SC block structure are illustrated in Fig. 1 (a) and Fig. 2 (a), respectively. Throughout the paper, the symbol-spaced discrete time representation is used. At the transmitter, a binary information sequence is data-modulated and then, the data-modulated symbol sequence is divided into a sequence of signal blocks of N_c symbols each, where N_c is the size of DFT at the receiver. The data symbol block is expressed using the vector form as $\mathbf{d}=[d(0), \dots, d(n), \dots, d(N_c-1)]^T$. The last N_g symbols of each block are copied as a CP and inserted into the guard interval (GI) placed at the beginning of each block and a CP-inserted data block of N_c+N_g symbols is transmitted.

The received signal block after CP removal is transformed by N_c -point DFT into the frequency-domain signal. Then, QRM-MLBD or MMSE QRM-MLBD is carried out to obtain the decision variable block.

B. TS-SC

The TS-SC block transmission system model and the TS-SC block structure are illustrated in Fig. 1 (b) and Fig. 2 (b), respectively. CP is replaced by TS. In order to let TS to play the role of CP, DFT size at the receiver must be the sum of number of useful data symbols and the TS length. In this paper, to keep the same data rate as CP-SC, the data symbol block length and the TS length need to be set to N_c and N_g , respectively. The difference between TA-SC and CP-SC is the size of DFT to be used at the receiver; the DFT size is N_c+N_g symbols for TA-SC while it is N_c symbols for CP-SC.

The data symbol block can be expressed similar to CP-SC as $\mathbf{d}=[d(0),\dots,d(n),\dots,d(N_c-1)]^T$. Before the transmission, the TS of length N_g symbols is appended at the end of each block. The block \mathbf{s} to be transmitted is expressed using the vector form as

$$\mathbf{s} = [s(0), \dots, s(N_c + N_g - 1)]^T = [d(0), \dots, d(N_c - 1), u(0), \dots, u(N_g - 1)]^T = \begin{bmatrix} \mathbf{d} \\ \mathbf{u} \end{bmatrix}, \quad (1)$$

where $\mathbf{u}=[u(0),\dots,u(n),\dots,u(N_g-1)]^T$ denotes the TS vector which is identical for all blocks.

The received signal block is transformed by N_c+N_g -point DFT into the frequency-domain signal. Then, TS-aided QRM-MLBD is carried out to obtain the decision variable block.

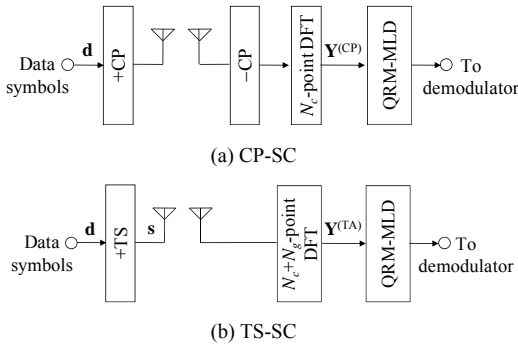


Fig. 1 Transmission system model.

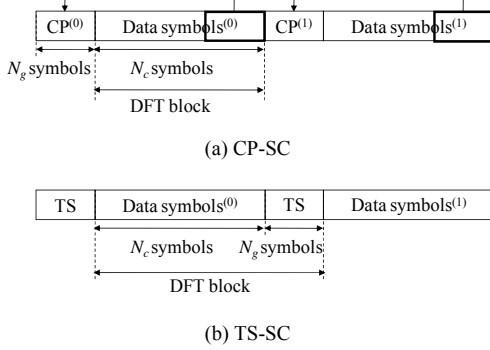


Fig. 2 Block structure.

III. QRM-MLBD FOR CP-SC

A. Received Signal

We assume a symbol-spaced frequency-selective block fading channel composed of L distinct propagation paths. The frequency-domain signal vector $\mathbf{Y}^{(\text{CP})}=[Y^{(\text{CP})}(0),\dots,Y^{(\text{CP})}(k),\dots,Y^{(\text{CP})}(N_c-1)]^T$ after an N_c -point DFT is expressed as [3]

$$\mathbf{Y}^{(\text{CP})} = \sqrt{\frac{2E_s}{T_s}} \mathbf{H}^{(\text{CP})} \mathbf{F}^{(N_c)} \mathbf{d} + \mathbf{N}^{(\text{CP})} = \sqrt{\frac{2E_s}{T_s}} \bar{\mathbf{H}}^{(\text{CP})} \mathbf{d} + \mathbf{N}^{(\text{CP})}, \quad (2)$$

where E_s and T_s are respectively the symbol energy and duration, $\mathbf{F}^{(J)}$ is the DFT matrix of size $J \times J$, $\mathbf{H}^{(\text{CP})}$ is the channel matrix, and $\mathbf{N}^{(\text{CP})}=[N^{(\text{CP})}(0),\dots,N^{(\text{CP})}(k),\dots,N^{(\text{CP})}(N_c-1)]^T$ is the frequency-domain noise vector. The k th element, $N^{(\text{CP})}(k)$, of $\mathbf{N}^{(\text{CP})}$ is the zero-mean additive white Gaussian noise (AWGN) having the variance $2N_0/T_s$ with N_0 being the one-sided noise power spectrum density. $\mathbf{H}^{(\text{CP})}$ is given as $\mathbf{H}^{(\text{CP})}=\text{diag}[H^{(\text{CP})}(0),\dots,H^{(\text{CP})}(k),\dots,H^{(\text{CP})}(N_c-1)]$, where $H^{(\text{CP})}(k)$ is the channel gain at the k th frequency and $\bar{\mathbf{H}}^{(\text{CP})}=\mathbf{H}^{(\text{CP})}\mathbf{F}^{(N_c)}$ is the equivalent channel matrix.

B. QRM-MLBD

In QRM-MLBD, QR decomposition is applied to the equivalent channel $\bar{\mathbf{H}}^{(\text{CP})}$ which is a concatenation of the propagation channel and DFT. First, applying the QR decomposition to the equivalent channel matrix $\bar{\mathbf{H}}^{(\text{CP})}$, we have $\bar{\mathbf{H}}^{(\text{CP})}=\mathbf{Q}^{(\text{CP})}\mathbf{R}^{(\text{CP})}$, where $\mathbf{Q}^{(\text{CP})}$ is an $N_c \times N_c$ matrix satisfying $\{\mathbf{Q}^{(\text{CP})}\}^H \mathbf{Q}^{(\text{CP})}=\mathbf{I}$ and $\mathbf{R}^{(\text{CP})}$ is an $N_c \times N_c$ upper triangular matrix. The transformed frequency-domain received signal $\hat{\mathbf{Y}}^{(\text{CP})}$ is obtained as

$$\hat{\mathbf{Y}}^{(\text{CP})} = \{\mathbf{Q}^{(\text{CP})}\}^H \mathbf{Y}^{(\text{CP})} = \sqrt{\frac{2E_s}{T_s}} \mathbf{R}^{(\text{CP})} \mathbf{d} + \{\mathbf{Q}^{(\text{CP})}\}^H \mathbf{N}^{(\text{CP})}. \quad (3)$$

From Eq. (3), the ML solution can be obtained by searching for the best path having the minimum Euclidean distance in the tree diagram composed of N_c stages. By utilizing tree structure, ML using M-algorithm [9] can be applied. An example of the ML using M-algorithm for CP-SC is shown in Fig. 3 (a) assuming $N_c=4$, BPSK modulation, and the number M of surviving paths is 3. In the first stage ($n=0$), all possible symbol-candidates for the last symbol $d(N_c-1)$ in a data symbol block are generated (the number of all possible symbol-candidates is X for X -QAM). The path metric based on the squared Euclidean distance between $\hat{Y}^{(\text{CP})}(N_c-1)$ and each symbol-candidate is calculated. Next, M ($M \leq X$) paths having the smallest path metric are selected as surviving paths. In the next stage ($n=1$), there are a total of X branches for $d(N_c-2)$ leaving from each selected surviving path. Therefore, there are totally $M \cdot X$ possible paths for the two symbol sequence of $d(N_c-1)$ and $d(N_c-2)$. The path metrics are calculated for all possible $M \cdot X$ paths. Similar to the first stage, M surviving paths are selected from $M \cdot X$ paths. This procedure is repeated until the last stage ($n=N_c-1$). The most possible transmitted symbol sequence is found by tracing back the path with the smallest path metric at the last stage. QRM-MLBD requires $X\{1+M(N_c-1)\}$ times squared Euclidean distance calculation, which is significantly smaller than the original MLBD that requires X^{N_c} times squared Euclidean distance calculation. However, in the case of CP-SC using the conventional QRM-MLBD, a fairly large M is required to achieve the sufficiently improved BER performance, leading to high computational complexity. The reason is stated below.

The received signal power associated with the symbol $d(N_c-1-i)$ at the n th stage ($n \geq i$, $n=0,1,\dots,N_c-1$) is the sum of

the squared values of the $(N_c-1), (N_c-2), \dots, (N_c-1-i)$ th elements in the (N_c-1-i) th column of $\mathbf{R}^{(\text{CP})}$. In the case of SC transmission, the magnitude of a lower right element of $\mathbf{R}^{(\text{CP})}$ drops with large probability [10]. This indicates that when small M is used, the probability of removing the correct paths at early stages increases. The selection error at early stages greatly affects the achievable BER performance since the MLD using the M-algorithm successively reduces the paths stage-by-stage. Therefore, to improve the BER performance, this probability must be reduced. If large M is used, this probability can be reduced, but at the cost of increased computational complexity.

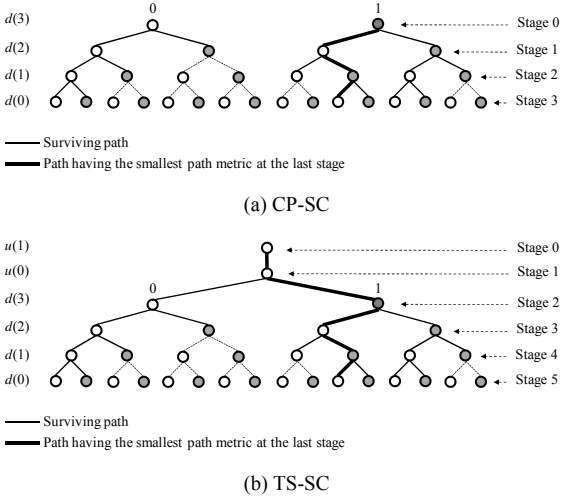


Fig. 3 MLD using M-algorithm ($M=3$) with BPSK.

C. MMSE QRM-MLBD

To reduce the number of surviving paths, we apply the MMSE QRM-MLBD, which was originally proposed for MIMO spatial multiplexing [5], to the CP-SC block transmission. In the MMSE QRM-MLBD, the drop in the magnitude of a lower right element of \mathbf{R} can be prevented by using the MMSE based QR decomposition [11]. As a result, it can be expected that the probability of removing the correct paths at an early stage will be reduced even if small M is used.

In the MMSE QRM-MLBD, first, we introduce a $2N_c \times N_c$ extended channel matrix $\bar{\mathbf{H}}^{\text{ext}}$ and a $2N_c \times 1$ extended frequency-domain received signal vector \mathbf{Y}^{ext} :

$$\bar{\mathbf{H}}^{\text{ext}} = \begin{bmatrix} \bar{\mathbf{H}} \\ \sqrt{N_0/E_s} \mathbf{I}_{N_c} \end{bmatrix}, \quad \mathbf{Y}^{\text{ext}} = \begin{bmatrix} \mathbf{Y} \\ \mathbf{0}_{N_c \times 1} \end{bmatrix}, \quad (4)$$

where \mathbf{I}_{N_c} is an $N_c \times N_c$ identity matrix and $\mathbf{0}_{N_c \times 1}$ is a zero column vector of length N_c . Next, applying the QR decomposition to the extended channel matrix $\bar{\mathbf{H}}^{\text{ext}}$, we have $\bar{\mathbf{H}}^{\text{ext}} = \tilde{\mathbf{Q}}\tilde{\mathbf{R}}$, where $\tilde{\mathbf{Q}}$ is a $2N_c \times N_c$ matrix satisfying $\tilde{\mathbf{Q}}^H \tilde{\mathbf{Q}} = \mathbf{I}$ and $\tilde{\mathbf{R}}$ is an $N_c \times N_c$ upper triangular matrix. The transformed frequency-domain received signal $\tilde{\mathbf{Y}}$ is obtained as

$$\tilde{\mathbf{Y}} = \tilde{\mathbf{Q}}^H \mathbf{Y}^{\text{ext}} = \sqrt{\frac{2E_s}{T_s}} \tilde{\mathbf{R}} \mathbf{d} + \tilde{\mathbf{Q}}^H \begin{bmatrix} \mathbf{N}^{(\text{CP})} \\ -\sqrt{N_0/E_s} \mathbf{d} \end{bmatrix}. \quad (5)$$

From Eq. (5), the ML solution is obtained by carrying out,

$$\hat{\mathbf{d}} = \arg \min_{\mathbf{d} \in X^{N_c}} \left\{ \left\| \tilde{\mathbf{Y}} - \sqrt{\frac{2E_s}{T_s}} \tilde{\mathbf{R}} \mathbf{d} \right\|^2 - \frac{N_0}{E_s} \|\mathbf{d}\|^2 \right\}, \quad (6)$$

where $\bar{\mathbf{d}}$ is a symbol-candidate vector. In MMSE QRM-MLBD, M-algorithm is applied to Eq. (6), in the same way as the conventional QRM-MLBD, except that there is one more term participating the path metric calculation when 16QAM and 64QAM is used (For 4QAM(QPSK), it is a constant and can be ignored).

IV. QRM-MLBD FOR TS-SC

A. Received Signal

In TS-SC, the frequency-domain signal vector $\mathbf{Y}^{(\text{TS})} = [Y^{(\text{TS})}(0), \dots, Y^{(\text{TS})}(k), \dots, Y^{(\text{TS})}(N_c+N_g-1)]^T$ after an N_c+N_g -point DFT is expressed as [8]

$$\mathbf{Y}^{(\text{TS})} = \sqrt{\frac{2E_s}{T_s}} \mathbf{H}^{(\text{TS})} \mathbf{F}^{(N_c+N_g)} \mathbf{s} + \mathbf{N}^{(\text{TS})} = \sqrt{\frac{2E_s}{T_s}} \bar{\mathbf{H}}^{(\text{TS})} \mathbf{s} + \mathbf{N}^{(\text{TS})}, \quad (7)$$

where $\mathbf{H}^{(\text{TS})} = \text{diag}[H^{(\text{TS})}(0), \dots, H^{(\text{TS})}(k), \dots, H^{(\text{TS})}(N_c+N_g-1)]$ is the channel matrix of size $(N_c+N_g) \times (N_c+N_g)$, $\mathbf{N}^{(\text{TS})} = [N^{(\text{TS})}(0), \dots, N^{(\text{TS})}(k), \dots, N^{(\text{TS})}(N_c+N_g-1)]^T$ is the frequency-domain noise vector, and $\bar{\mathbf{H}}^{(\text{TS})} = \mathbf{H}^{(\text{TS})} \mathbf{F}^{(N_c+N_g)}$ is the equivalent channel matrix in the case of TS-SC.

B. TS-aided QRM-MLBD

In the case of TS-SC, QR decomposition is applied to the equivalent channel $\bar{\mathbf{H}}^{(\text{TS})}$ in the same way as CP-SC. The QR decomposition is applied to the equivalent channel matrix $\bar{\mathbf{H}}^{(\text{TS})}$ to obtain $\bar{\mathbf{H}}^{(\text{TS})} = \mathbf{Q}^{(\text{TS})} \mathbf{R}^{(\text{TS})}$, where $\mathbf{Q}^{(\text{TS})}$ is an $(N_c+N_g) \times (N_c+N_g)$ matrix satisfying $\mathbf{Q}^{(\text{TS})H} \mathbf{Q}^{(\text{TS})} = \mathbf{I}$ and $\mathbf{R}^{(\text{TS})}$ is an $(N_c+N_g) \times (N_c+N_g)$ upper triangular matrix. The transformed frequency-domain received signal is obtained as

$$\hat{\mathbf{Y}}^{(\text{TS})} = \{\mathbf{Q}^{(\text{TS})}\}^H \mathbf{Y}^{(\text{TS})} = \sqrt{\frac{2E_s}{T_s}} \mathbf{R}^{(\text{TS})} \begin{bmatrix} \mathbf{d} \\ \mathbf{u} \end{bmatrix} + \{\mathbf{Q}^{(\text{TS})}\}^H \mathbf{N}^{(\text{TS})}. \quad (8)$$

From Eq. (8), the ML solution can be obtained by searching for the best path having the minimum Euclidean distance in the tree diagram composed of N_c+N_g stages. However, in TS-SC, the $N_c, N_c+1, \dots, (N_c+N_g-1)$ th elements of $\hat{\mathbf{Y}}^{(\text{TS})}$ contain the training symbols only and therefore, only one path exists at the $n=0, 1, \dots, (N_g-1)$ th stages as shown in Fig. 3 (b) (assuming $N_c=4, N_g=2$, BPSK modulation, and the number M of surviving paths is 3). Therefore, in the case of TS-SC, the lower right elements of $\mathbf{R}^{(\text{TS})}$ are associated with TS and therefore, they are not relevant to the selection of the surviving path. The MLD using M-algorithm can start from

the $n=N_g$ th stage and therefore, the probability of removing the correct path at early stages can be significantly reduced even if small M is used. It should be noted that the MMSE QRM-MLBD also can be used in the case of TS-SC. However, in this paper, we use only the conventional QRM-MLBD because the performance of MMSE QRM-MLBD is almost the same as the conventional QRM-MLBD in the case of TS-SC.

V. COMPUTER SIMULATION

The simulation condition is summarized in Table I. The data symbol block length is $N_c=64$ for both CP- and TS-SC and the TS length of TS-SC is $N_g=16$ which is equal to the CP length of CP-SC. A partial sequence taken from a PN sequence with a repetition period of 4095 bits is used as TS. The same data modulation is used for TS and useful data. The channel is assumed to be a frequency-selective block Rayleigh fading channel having symbol-spaced 16-path uniform power delay profile. Ideal channel estimation is assumed.

TABLE I Computer simulation condition

Transmitter	Data modulation	QPSK, 16QAM
	Data symbol block length	$N_c=64$
	TS and CP lengths	$N_g=16$
Channel	Fading type	Frequency-selective block Rayleigh
	Power delay profile	$L=16$ path uniform power delay profile
	Time delay	$\tau=l$ ($l=0\sim L-1$)
Receiver	Channel estimation	Ideal

The BER performances of CP-SC using QRM-MLBD, CP-SC using MMSE QRM-MLBD, and TS-SC using TS-aided QRM-MLBD are plotted in Fig. 4 as a function of average received bit energy-to-noise power spectrum density ratio $E_b/N_0(=(E_s/N_0)(1+N_g/N_c)/\log_2 X)$. For comparison, the MF bound [12] is also plotted. It can be seen from Fig. 4 that when small M is used, the achievable BER performance of CP-SC using QRM-MLBD degrades. On the other hand, CP-SC using MMSE QRM-MLBD and TS-SC using TS-aided QRM-MLBD can achieve better BER performance even if small M is used. When QPSK is used, CP-SC using MMSE QRM-MLBD and TS-SC using TS-aided QRM-MLBD can achieve almost the same BER performance. On the other hand, when 16QAM is used, TS-SC using TS-aided QRM-MLBD can achieve better BER performance than CP-SC using MMSE QRM-MLBD.

We also compare the conventional QRM-MLBD, MMSE QRM-MLBD, and TS-aided QRM-MLBD in terms of the computational complexity. The complexity here is defined as the number of complex multiplications per block, which is the sum of the complexity required for DFT, QR decomposition, multiplication of \mathbf{Q}^H , and the squared Euclidean distance

calculation. The required number of complex multiplications is shown in Table II.

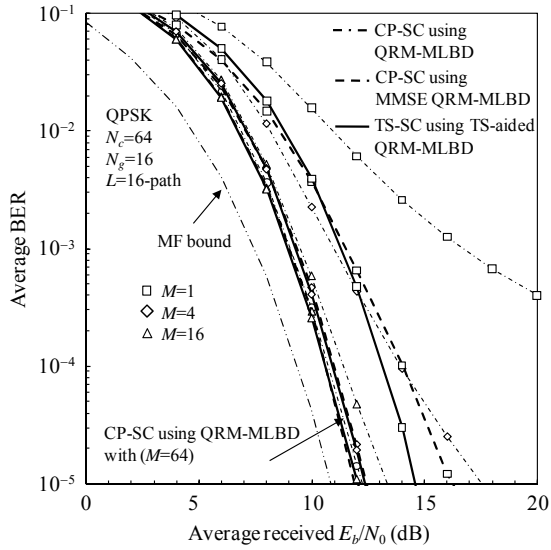
Figure 5 plots the required number of complex multiplications per block for the conventional QRM-MLBD, MMSE QRM-MLBD, and TS-aided QRM-MLBD as a function of the required average received E_b/N_0 for achieving $\text{BER}=10^{-3}$. The relationship between required number of complex multiply operations and required average received E_b/N_0 is varied by changing the value of M ($M=1\sim 256$). For comparison, the relationship between required number of complex multiplications and required average received E_b/N_0 of MMSE-FDE and required average received E_b/N_0 of MF bound also plotted. In the case of the conventional QRM-MLBD, the required value of M to achieve the BER performance close to the MF bound is 64 for QPSK and 256 for 16QAM (The performance gap of 1dB from the MF bound is owing to the insertion of TS or CP). However, in the case of MMSE QRM-MLBD, smaller M is required, i.e., $M=8$ for QPSK and 64 for 16QAM. As a result, the computational complexity for MMSE QRM-MLBD is smaller than that of the conventional QRM-MLD. When QPSK (16QAM) is used, the computational complexity in MMSE QRM-MLBD is about 74(30) % of that in the conventional QRM-MLBD.

TS-aided QRM-MLBD can further reduce the required value of M when 16QAM is used, i.e., $M=8$ for QPSK and 8 for 16QAM. When QPSK is used, TS-aided requires almost the same complexity as MMSE QRM-MLBD. On the other hand, when 16QAM is used, the computational complexity for TS-aided QRM-MLBD is much smaller than that of MMSE QRM-MLBD. When QPSK (16QAM) is used, the computational complexity in TS-aided QRM-MLBD is about 77(10) % of that in the conventional QRM-MLBD.

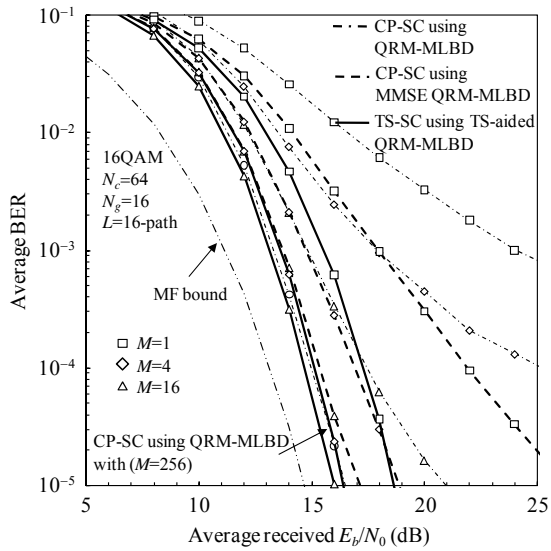
Finally, we discuss the comparison between proposed QRM-MLBDs and MMSE-FDE. Proposed QRM-MLBDs can significantly reduce the required E_b/N_0 compared to MMSE-FDE. However, the computational complexity of proposed QRM-MLBD is still higher than MMSE-FDE. This is because QR decomposition requires high computational complexity. Therefore, further complexity reduction is necessary. This is left as an interesting future research topic.

V. CONCLUSION

In this paper, we compared our previously proposed complexity reduced QRM-MLBDs in terms of the BER performance and computational complexity. We showed that both MMSE QRM-MLBD and TS-aided QRM-MLBD can achieve better BER performance even if small M is used. Therefore, the computational complexity required for signal detection is greatly reduced. When QPSK is used, the complexity required for MMSE QRM-MLBD is about 74% of that in the conventional QRM-MLBD. When 16QAM is used, the complexity required for TS-aided QRM-MLBD is about 10% of that in the conventional QRM-MLBD.



(a) QPSK



(b) 16QAM

Fig. 4 Average BER performance.

TABLE II Number of multiplications

	CP-SC using QRM-MLD	CP-SC using MMSE QRM-MLD	TA-SC using QRM-MLD
DFT	$N_c^2(N_c \log_2 N_c)$	$N_c^2(N_c \log_2 N_c)$	$(N_c + N_g)^2$
QR decomposition	N_c^3	$2N_c^2$	$(N_c + N_g)^3$
Multiplication of \mathbf{Q}^H	N_c^2	N_c^2	$(N_c + N_g)^2$
Squared Euclidian distance calculations	$2X + \sum_{i=1}^{N_c-1} (i+2)$	$2X + \sum_{i=1}^{N_c-1} (i+2)$	$(2+N_g)X + \sum_{i=1}^{N_c-1} (i+2+N_g)$

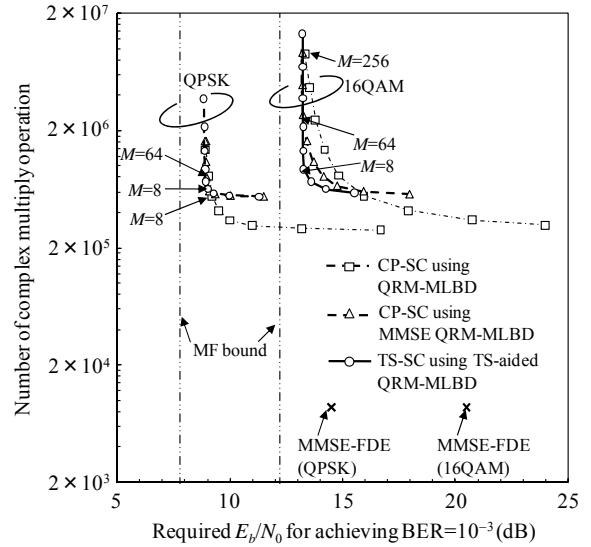


Fig. 5 Required E_b/N_0 versus computational complexity.

REFERENCES

- [1] J. G. Proakis and M. Salehi, *Digital communications*, 5th ed., McGraw-Hill, 2008.
- [2] K. Nagatomi, K. Higuchi, and H. Kawai, "Complexity reduced MLD based on QR decomposition in OFDM MIMO multiplexing with frequency domain spreading and code multiplexing," in Proc. IEEE Wireless Communications and Networking Conference (WCNC 2009), pp. 1-6, Apr. 2009.
- [3] T. Yamamoto, K. Takeda, and F. Adachi, "Single-carrier transmission using QRM-MLD with antenna diversity," in Proc. The 12th International Symposium on Wireless Personal Multimedia Communications (WPMC 2009), Sep. 2009.
- [4] D. Falconer, S. L. Ariyavisitakul, A. Benyamini-Seeyar, and B. Edison, "Frequency domain equalization for single-carrier broadband wireless systems," *IEEE Commun. Mag.*, Vol. 40, No. 4, pp. 58-66, Apr. 2002.
- [5] S. Sun, Y. Dai, Z. Lei, K. Higuchi, and H. Kawai, "Pseudo-inverse MMSE based QRD-M algorithm for MIMO OFDM," in Proc. The IEEE 63rd Vehicular Technology Conference (VTC-Spring), May. 2006.
- [6] T. Yamamoto, K. Takeda, and F. Adachi, "MMSE based QRM-MLD frequency-domain block signal detection for single-carrier transmission," in Proc. 7th IEEE VTS Asia Pacific Wireless Communication Symposium (APWCS 2010), May 2010.
- [7] T. Yamamoto, K. Takeda, and F. Adachi, "Training Sequence-aided Single-carrier Block Signal Detection Using QRM-MLD," in Proc. IEEE Wireless Communications and Networking Conference (WCNC 2010), pp. 1-6, Apr. 2010.
- [8] L. Deneire, B. Gyselinckx, and M. Engels, "Training sequence versus cyclic prefix - a new look on single carrier communication," *IEEE Commun. Lett.*, Vol. 5, No. 7, pp. 292-294, Jul. 2001.
- [9] J. B. Anderson and S. Mohan, "Sequential coding algorithms: A survey and cost analysis," *IEEE Trans. on Commun.*, Vol. 32, pp. 169-176, Feb. 1984.
- [10] K. Takeda, H. Tomeba, and F. Adachi, "Joint Tomlinson-Harashima precoding and frequency-domain equalization for broadband single-carrier transmission," *IEICE Trans. Commun.*, Vol. E91-B, No. 1, pp. 258-266, Jan. 2008.
- [11] D. Wubben, R. Bohnke, V. Kuhn, and K. D. Kammeyer, "MMSE extension of V-BLAST based on sorted QR decomposition," in Proc. The IEEE 58th Vehicular Technology Conference (VTC-Fall), Oct. 2003.
- [12] F. Adachi and K. Takeda, "Bit error rate analysis of DS-SS-CDMA with joint frequency-domain equalization and antenna diversity combining," *IEICE Trans. Commun.*, Vol. E87-B, No. 10, pp.2991-3002, Oct. 2004.